Picosecond Forward Electron Transfer and Nanosecond Back Electron Transfer in an Azacrown-Substituted $[(bpy)Re(CO)_3(L)]^+$ Complex: Direct Observation by Time-Resolved UV−Visible Absorption Spectroscopy

Jared D. Lewis,[†] Laura Bussotti,[‡] Paolo Foggi,[‡,§] Robin N. Perutz,[†] and John N. Moore*[,†]

Department of Chemistry, The University of York, Heslington, York, YO10 5DD, U.K., LENS, via Nello Carrara 1, and INFM Unita' di Firenze, via Giovanni Sansone 1, Polo Scientifico, 50019 Sesto F.no, Florence, Italy, and Department of Chemistry, University of Perugia, via Elce di Sotto 8, 06100 Perugia, Italy

Received: August 22, 2002; In Final Form: October 21, 2002

Intramolecular electron transfer in the excited state of a $[(bpy)Re^{I}(CO)_3(L)]^+$ complex (bpy = 2,2′-bipyridine), in which L contains a pendant azacrown ether that acts as an electron donor (L = *N*-[4-(4,7,10,13-tetraoxa-1-azacyclopentadecyl)benzoyl]-4-aminopyridine), has been studied directly using picosecond and nanosecond time-resolved UV−visible absorption spectroscopy. Picosecond studies show that the metal-to-ligand charge-transfer (MLCT) state produced on excitation, $[(bpy^{\bullet-})Re^{II}(CO)_3(L)]^+$, undergoes forward electron transfer with a rate constant of $k_{FET} = 2.0 \times 10^9$ s^{-1} to generate a ligand-to-ligand charge-transfer (LLCT) state, $[(bpy^{\bullet-})Re^{I}(CO)_3(L^{\bullet+})]^+$, in which the metal has been reduced back to Re(I) and charge separation has been effected between the bipyridine and azacrown ligands. Nanosecond studies show that the LLCT state returns to the ground state by back electron transfer from the bipyridine to azacrown ligand, with a rate constant of $k_{BET} = 5.3 \times 10^7$ s^{-1}. Studies of complexes in which the azacrown complex is protonated, or is absent, demonstrate that intramolecular electron transfer to form the LLCT state does not occur in these cases. Forward electron transfer in the azacrown complex takes place on the picosecond time scale: it is weakly exoergonic and occurs in the Marcus normal region, with electronic coupling between the azacrown ligand and the rhenium metal center of ca. 100 cm^{-1}. Back electron transfer takes place on the nanosecond time scale: it is strongly exoergonic and occurs in the Marcus inverted region, with much weaker electronic coupling between the bipyridine and azacrown ligands. The rapid formation of a long-lived charge-separated state indicates that this molecule has a suitable design for a photochemical device.

Introduction

Interest in photoinduced electron-transfer reactions is stimulated by the prospect of photochemical devices such as sensors, switches, or redox agents.[1,2] A detailed understanding of excited-state electron-transfer dynamics, and how they are affected by molecular structure, is particularly important for the informed design of supramolecular systems that contain several functional groups, and that offer a wide variety of opportunities to act as devices. Photoinduced electron-transfer reactions occur in many covalently linked donor−acceptor molecules containing one or more photoactive metal centers, such as polypyridyl complexes of Ru(II), Os(II), Re(I), and recently Pt(II).[3−14] In these examples, either two metal centers[3−8] or a metal center and an organic molecule[9−14] constitute the donor−acceptor pair, with an organic spacer such as a phenylene chain[3] or an oligopeptide[4,5,10,12] typically linking the donor and acceptor groups. Systematic studies of electron-transfer rates as a function of molecular structure enable the effects of donor−acceptor redox potential and electronic coupling via the spacer group to be rationalized.[4−7,10,12,13]

Complexes of the type $(N-N)Re(CO)_3(X)$ (X = halide, N-donor, etc.), where N−N is a diimine ligand such as 2,2′-bipyridine or 1,10-phenanthroline, generally possess $d\pi(Re) \rightarrow \pi^*(N-N)$ metal-to-ligand charge-transfer (MLCT) lowest excited states that are luminescent, relatively long-lived (lifetimes typically of 10 ns to 100 μs), and able to undergo both reduction and oxidation reactions more readily than the ground states.[15,16] Consequently, these complexes readily undergo MLCT excited-state quenching, either by intermolecular electron transfer with an appropriate donor or acceptor in solution,[15] or by intramolecular electron transfer if an appropriate donor or acceptor is present within an attached ligand.[13,17] The versatility of these $(N-N)Re(CO)_3(L)$ complexes has resulted in their increasing use as components within supramolecular donor−acceptor systems. In several examples where L is an organic ligand containing a pendant electron donor, intramolecular electron transfer in the MLCT state has been shown to create a ligand-to-ligand charge-transfer (LLCT) state in which the positive and negative charge equivalents are localized on the L and N−N ligands, respectively, as illustrated in Scheme 1.[13,17−19] To create useful photochemical devices based on intramolecular electron transfer in these rhenium complexes, it is desirable that the

SCHEME 1

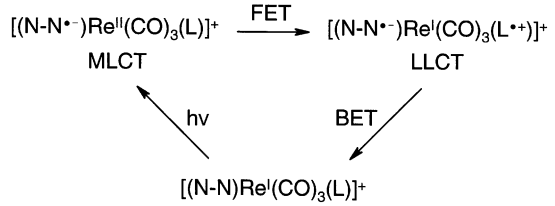

[†] The University of York.
[‡] LENS and INFM Unita' di Firenze.
[§] University of Perugia.

10.1021/jp021947l CCC: $22.00
Published on Web 11/28/2002

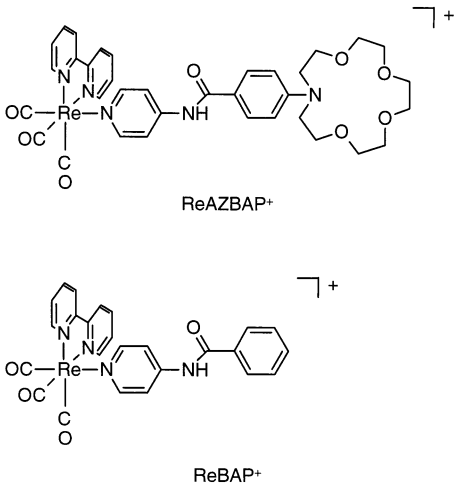

Figure 1. Structures of the ReAZBAP$^+$ and ReBAP$^+$ complexes.

MLCT state undergoes rapid forward electron transfer (FET) to create a charge-separated LLCT state, and that this LLCT state is relatively long-lived, undergoing slow back electron transfer (BET) to return to the ground state.

Forward electron transfer occurs on the nanosecond time scale in the MLCT states of several [(N−N)Re(CO)$_3$(L)]$^+$ complexes where L contains a pendant amine electron donor, with rate constants derived from a combination of the MLCT emission lifetime of the electron-donor complex and the longer MLCT emission lifetime of a suitable model complex in which electron-transfer quenching does not occur.[13,17] Back electron transfer in the LLCT state usually occurs on a longer time scale than forward electron transfer in the MLCT state, with rate constants obtained by conventional nanosecond time-resolved UV−visible absorption (TRVIS) techniques because the LLCT states are not emissive.[13,17,20] Forward electron transfer in some [(N−N)-Re(CO)$_3$(L)]$^+$ complexes may occur on a time scale of <10 ns,[13,21] but few direct studies of forward and back electron transfers have been reported for such complexes because of the ultrafast time resolution required.

One direct study of ultrafast electron transfer has been reported for the MLCT state of [(dmb)Re(CO)$_3$(MQ$^+$)]$^+$ (where dmb = 4,4′-dimethyl-2,2′-bipyridine and MQ$^+$ = 4-methyl-4,4′-bipyridinium).[21] In this case, the FET process is different from the ligand-to-metal electron transfer in Scheme 1 and instead involves ligand-to-ligand electron transfer: a transient absorption spectrum assigned to a dmb-localized MLCT state has been observed to evolve into a spectrum assigned to a MQ-localized MLCT state as electron transfer occurs from the dmb ligand to the MQ$^+$ ligand. This MLCT(dmb) → MLCT(MQ) process was found to have a lifetime of 8.3 ps in acetonitrile, arising from forward electron transfer in the Marcus normal region.

Ultrafast electron transfer of the type shown in Scheme 1 was proposed by MacQueen and Schanze for a [(bpy)Re(CO)$_3$-(L)]$^+$ complex (ReAZBAP$^+$; Figure 1), in which L contains an azacrown ether linked to the rhenium center by an organic connector incorporating an amide group, on the basis of time-resolved emission studies.[22] The MLCT emission of this complex was found to be weak and short-lived (<1 ns), and it was proposed that electron transfer occurs from the azacrown nitrogen atom to the rhenium center to generate a LLCT state on the ultrafast time scale. A novel feature of ReAZBAP$^+$ was the increase in emission yield that was reported to be induced either by adding acid, or by adding alkali or alkaline-earth metal salts, with the magnitude of the increase dependent on the cation; this effect was proposed to arise from inhibition of forward electron transfer in the MLCT state by the binding of a proton to the lone pair of the azacrown nitrogen atom or by the binding of a metal cation within the azacrown.

The cation-regulated photophysics of ReAZBAP$^+$ reported by MacQueen and Schanze are potentially very interesting for further study. First, it was proposed that forward electron transfer occurs rapidly in the MLCT state to create a LLCT state; and, by comparison with similar complexes,[13] such an LLCT state would be expected to be relatively long-lived. Hence, this complex may provide a long-lived charge-separated state that is desirable in photochemical devices. Second, it was proposed that the emission yield of the metal-bound complexes, ReAZBAP$^+$−M^{n+}, was lower than that of the protonated complex, ReAZBAP$^+$−H$^+$, because of metal cation ejection in the MLCT state. Although the proposed cation ejection may limit the effectiveness of this complex as a metal-cation sensor,[22] it may offer the possibility for its application as a light-controlled metal-cation switch.

In this paper, we present picosecond and nanosecond time-resolved UV−visible absorption and emission studies of the ReAZBAP$^+$ complex in the absence of cations, of the protonated form, ReAZBAP$^+$−H$^+$, and of two model complexes ReBAP$^+$ (Figure 1) and (bpy)Re(CO)$_3$Cl (abbreviated here as ReCl) in which the ligands attached to (bpy)Re(CO)$_3$ do not contain a pendant electron donor. The aim of this work was to observe the MLCT and proposed LLCT states of ReAZBAP$^+$ directly by time-resolved UV−visible absorption spectroscopy, to determine the dynamics of the proposed forward and reverse electron-transfer reactions, to study the effect of protonating the azacrown, and to establish the photophysical properties of ReAZBAP$^+$ prior to testing its application as a cation switch. This study extends our work on the photophysics and photochemistry of organic and organometallic azacrown compounds that can act as photochemical cation switches;[23−26] our TRVIS studies of ReAZBAP$^+$−M^{n+} complexes will be reported separately because they have revealed significantly more complicated processes than those observed in the absence of metal cations.

Experimental Section

The ligands AZBAP[22] and BAP[22] (*N*-benzoyl-4-aminopyridine) and the complexes [ReAZBAP]PF$_6$,[22] [ReBAP]PF$_6$,[22] and ReCl,[15] were prepared according to literature methods and characterized using ^{1}H NMR and ESI-MS. Thionyl chloride was distilled from triphenyl phosphite (both Aldrich); Re$_2$(CO)$_{10}$ (Strem), phenyl-aza-15-crown ether (Acros), and all other materials (Aldrich) were used as received.

UV−visible absorption spectra were recorded using a Hitachi U-3000 spectrophotometer with matched quartz cells of path length 1 mm or 1 cm. Corrected emission and excitation spectra were recorded using a Jobin-Yvon FluoroMax-2 spectrofluorometer with right-angle collection geometry and a 1 cm path length quartz cell.

For the nanosecond time-resolved UV−visible studies, samples were excited using single pulses of the third harmonic output (355 nm, 10 ns fwhm, 5−10 mJ/pulse) from a Q-switched Nd:YAG laser (Quanta-Ray GCR-3). The probe beam for transient absorption studies was provided by a pulsed 250 W Xe arc lamp; time-resolved emission was monitored in the absence of the probe beam. The transmitted or emitted light was analyzed with a monochromator and detected with a photomultiplier tube (Hamamatsu R928) linked to a 500 MHz digital oscilloscope (Tektronix TD520). The samples were contained in cells of path length 0.2 or 1.0 cm, at a concentration (10^{-5}−10^{-3} mol dm^{-3}) which gave an absorbance of ca. 0.5 at 355 nm, and were

degassed with several freeze−pump−thaw cycles. Data were collected as kinetic traces averaged over 16 laser pulses at a particular probe wavelength. Kinetic traces were converted to a time-dependent change in absorbance, ΔA_t, according to $\Delta A_t = \log(I_0/I_t)$. The traces were obtained as 5000-point datasets and were then averaged over 9 points to provide 556-point datasets for analysis; this averaging also effectively smoothed the data. Transient spectra were derived from kinetic traces recorded over a range of wavelengths; the kinetic traces were averaged over five points around a given delay time to obtain ΔA values that were plotted versus wavelength.

For the ultrafast time-resolved experiments,[27,28] a Ti:sapphire laser (Spectra Physics Tsunami) linked to an OPG/OPA system supplied excitation pulses (400 nm, ca. 100 fs) at a repetition rate of 1 kHz and with a pulse energy of 3 μJ at the sample. The probe pulses were provided by a white light continuum (300−1400 nm) generated by passing a portion of the Ti:sapphire laser output (800 nm, 1−2 mW) through an $x-y$ translating CaF_2 plate; the relative polarization of the pump and probe beams at the sample was set at the "magic angle" of 54.7°. The continuum beam was split into two: one portion was passed through the sample at a delay time controlled by an optical delay line, providing the probe pulse; the other portion was passed through the sample before the excitation pulse, providing a reference pulse for normalization. The continuum pulses were analyzed with a spectrograph (Chromex 250) and detected with a CCD detector (Princeton Instruments; 1100 × 330 pixels). Data were collected as transient spectra, typically with 50 spectra acquired at delay times from −10 ps to 2 ns. Transient kinetics were derived from these sets of transient spectra; each spectrum in a set was integrated over a range of 5 nm at a given wavelength, and the ΔA values were plotted versus delay time. The samples were prepared at a concentration (ca. 10^{-3} mol dm^{-3}) that gave an absorbance of ca. 1.0 at 400 nm and were contained in a cell of path length 1.8 mm that was translated rapidly in two directions perpendicular to the laser beams at a rate sufficient to ensure that each pulse sequence encountered fresh sample.

Kinetic traces were fitted to single- or multiexponential functions with offsets where appropriate, using either the SPSS software package (Statistical Package for the Social Sciences, SPSS Inc.) to fit at times outside the instrument response function, or in-house software that enabled analysis at all times by convolution of the model expression with the instrument response function. Lifetimes ($\tau = 1/k$) were obtained with uncertainties of 5−10% (nanosecond data) and 20% (ultrafast data).

Results

Steady-State UV−Visible Spectroscopy. The steady-state UV−visible absorption spectra of $ReAZBAP^+$, $ReAZBAP^+-H^+$, and $ReBAP^+$ in acetonitrile are shown in Figure 2. Band positions and absorption coefficients are listed in Table 1. The steady-state UV−visible emission spectra of all of the complexes showed an emission band at ca. 600 nm with a corresponding absorption band at ca. 350 nm observed in all of the excitation spectra.

Ultrafast Time-Resolved UV−Visible Spectroscopy. Ultrafast TRVIS spectra recorded on 400 nm excitation of $ReAZBAP^+$, $ReAZBAP^+-H^+$, $ReBAP^+$, and ReCl in acetonitrile are shown in Figure 3, along with kinetic traces. The TRVIS spectra of all of the complexes have a similar profile at 50 ps, with a moderately intense, broad band at ca. 400−600 nm. The TRVIS spectra of $ReAZBAP^+-H^+$, $ReBAP^+$, and ReCl showed no change over ca. 2 ns; the kinetics showed an instrument-limited rise and essentially no decay on this time scale. By contrast, the TRVIS spectrum of $ReAZBAP^+$ evolved over ca. 2 ns to give a spectrum with a stronger and sharper band at 500 nm; the TRVIS kinetics of $ReAZBAP^+$, recorded at 450−550 nm, showed an initial instrument-limited rise followed by a slower rise time of 500 ps, corresponding to the evolution of the sharper 500 nm band.

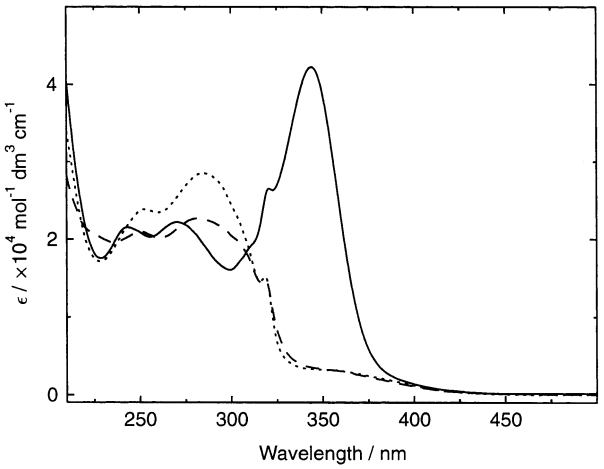

Figure 2. UV−visible absorption spectra of (—) $ReAZBAP^+$, (- - -) $ReAZBAP^+-H^+$, and (•••) $ReBAP^+$ (ca. 2×10^{-5} mol dm^{-3}) in acetonitrile. $ReAZBAP^+-H^+$ was produced by addition of excess HCl.

TABLE 1: UV−Visible Absorption Maxima (λ_{max}/nm) and Absorption Coefficients (ϵ_{max}/dm^3 mol^{-1} cm^{-1}) of the Complexes in Acetonitrile

	MLCT		IL	
complex	λ_{max}	ϵ_{max}	λ_{max}	ϵ_{max}
$ReAZBAP^+$	*a*		344	42000
$ReAZBAP^+-H^+$	350[b]	4000	281	22000
$ReBAP^+$	350[b]	4000	285	28000
ReCl	385	4500	290	23000

[a] Obscured. [b] Shoulder.

Nanosecond Time-Resolved UV−Visible Spectroscopy. Nanosecond TRVIS spectra recorded on 355 nm excitation of $ReAZBAP^+$, $ReAZBAP^+-H^+$, $ReBAP^+$, and ReCl in acetonitrile are shown in Figure 4, along with time-resolved absorption and emission kinetic traces. The nanosecond TRVIS spectra of $ReAZBAP^+-H^+$, $ReBAP^+$, and ReCl have a similar profile, comprising a strong, sharp band at 370 nm and weaker absorption at 400−600 nm. The TRVIS kinetics of these samples were found to fit well to monoexponential decays with lifetimes of 138, 145, and 22 ns for $ReAZBAP^+-H^+$, $ReBAP^+$, and ReCl, respectively (Table 2). The emission kinetics, recorded at ca. 600 nm, were also found to fit well to monoexponential decays with lifetimes that were the same as those measured by absorption, within experimental error. By contrast, the nanosecond TRVIS spectrum of $ReAZBAP^+$ consists of a broad band with a peak at 500 nm; strong ground-state absorption precluded the measurement of TRVIS data of $ReAZBAP^+$ below ca. 390 nm. The TRVIS kinetics of $ReAZBAP^+$ were found to fit well to a monoexponential decay with a lifetime of 19 ns. The time-resolved emission of $ReAZBAP^+$ was very short-lived, and a lifetime could not be obtained with the nanosecond apparatus.

Discussion

Steady-State Spectra. The steady-state absorption spectra of $ReBAP^+$ and ReCl (Figure 2) comprise moderately strong

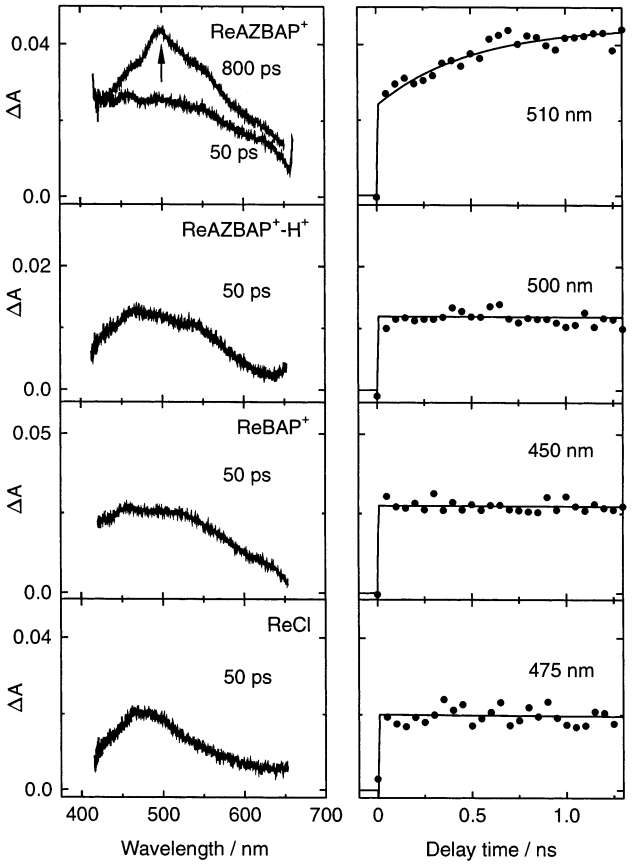

Figure 3. Ultrafast TRVIS spectra (left) obtained on 400 nm excitation of the complexes in acetonitrile, with delay times as indicated. Corresponding TRVIS kinetics (right), with probe wavelengths as indicated and the data points overlaid with solid lines which show fits (see text) comprising an instrument-limited rise as well as an additional rise of 500 ps for ReAZBAP$^+$, a decay of 138 ns for ReAZBAP$^+$−H$^+$, a decay of 145 ns for ReBAP$^+$, and a decay of 22 ns for ReCl.

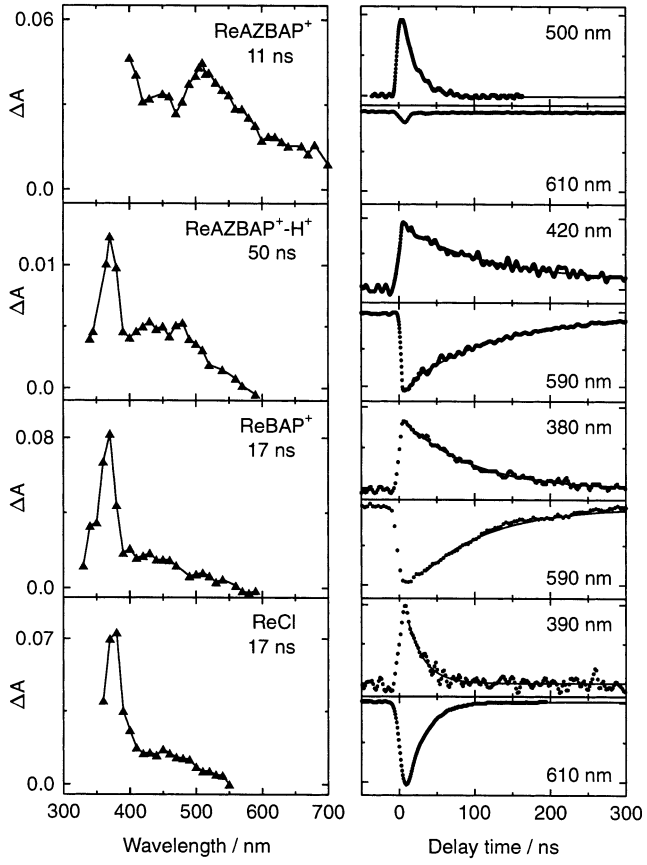

Figure 4. Nanosecond TRVIS spectra (left) obtained on 355 nm excitation of the complexes in acetonitrile, with delay times as indicated. Corresponding kinetics (right) as monitored by UV−visible absorption (upper in each case) and emission (lower in each case), with probe wavelengths as indicated and the data points overlaid with solid lines which show fits (see text) comprising a decay of 19 ns for ReAZBAP$^+$ (absorption only), 138 ns for ReAZBAP$^+$−H$^+$, 145 ns for ReBAP$^+$, and 22 ns for ReCl.

bands at <300 nm, assigned to intraligand (IL) $\pi \rightarrow \pi^*$ transitions localized on the bipyridine and BAP ligands, and a weaker band at ca. 350 nm assigned to the Re (dπ^*) → bpy (π^*) metal-to-ligand charge-transfer (MLCT) transition.[22] The absorption spectrum of ReAZBAP$^+$ comprises bpy- and AZBAP-localized IL bands at <300 nm, which are similar to those of ReBAP$^+$ and ReCl, and a strong band at 344 nm assigned to an intraligand charge-transfer (ILCT) transition in which charge is transferred from the amine electron donor to the amidopyridyl electron acceptor.[22] The ILCT band of ReAZBAP$^+$ is similar to that of the free AZBAP ligand,[29] although it is shifted to longer wavelength by 20 nm and has an absorption coefficient that is ca. 2.5 times stronger in the rhenium complex. The absorption spectrum of ReAZBAP$^+$−H$^+$ is similar to that of the ReBAP$^+$ model complex: the ILCT absorption band is lost on protonation of the azacrown nitrogen atom.

The steady-state emission spectra of all of the complexes give a band at ca. 600 nm assigned to emission from the MLCT excited state,[22] and the excitation spectra give a corresponding MLCT absorption band at ca. 350 nm. Notably, the MLCT excitation spectrum of ReAZBAP$^+$ gives a profile that is similar to that of the other complexes, confirming that its MLCT absorption band underlies the stronger ILCT band. The similarity in the absorption coefficients of ReAZBAP$^+$ and all of the other complexes at >390 nm (Figure 1) indicates that excitation of ReAZBAP$^+$ at >390 nm populates the MLCT excited state predominantly, whereas excitation of ReAZBAP$^+$ at 320−390 nm populates both MLCT and ILCT states.

TABLE 2: MLCT and LLCT Excited-State Lifetimes (ns) of the Complexes in Acetonitrile

complex	MLCT	LLCT
ReAZBAP$^+$	0.5	19
ReAZBAP$^+$−H$^+$	138	
ReBAP$^+$	145	
ReCl	22	
ReDMAB$^+$ [a]	11	77

[a] From ref 13.

ReBAP$^+$ Photophysics. The time-resolved absorption and emission data indicate that one excited state is observed on MLCT excitation of ReBAP$^+$. The TRVIS spectrum of ReBAP$^+$ at 50 ps (Figure 3) is similar to that at 17 ns (Figure 4). The ultrafast TRVIS kinetics show that the excited state forms directly on excitation, and the nanosecond TRVIS and emission kinetics show that it decays with a lifetime of 145 ns. The spectra reported here for ReBAP$^+$ are similar to those established for the MLCT state of ReCl, also shown here for comparison, and enable the TRVIS spectrum of ReBAP$^+$ to be assigned to the MLCT excited state.[15,16] The ReBAP$^+$ MLCT state lifetime of 145 ns agrees with the reported value[22] and is consistent with MLCT excited-state lifetimes for similar complexes.[15]

ReAZBAP$^+$ Photophysics. The time-resolved absorption and emission data indicate that two excited states are observed on excitation of ReAZBAP$^+$. Excitation at 400 nm, in the ultrafast experiment, populates the MLCT state exclusively. The TRVIS

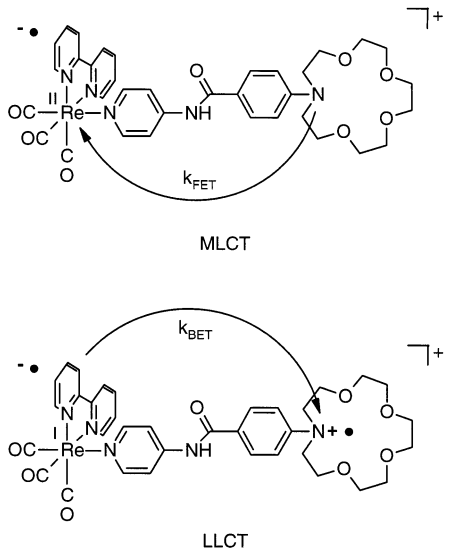

Figure 5. Forward and back electron transfers in ReAZBAP$^+$.

spectrum of ReAZBAP$^+$ at 50 ps is similar to that observed for ReBAP$^+$ (Figure 3), and it has an instrument-limited rise time: it can therefore be assigned to the MLCT excited state. The change in the TRVIS spectrum of ReAZBAP$^+$ (Figure 3) indicates that the MLCT state has a lifetime of 500 ps, converting to a longer-lived excited state; the very weak and short-lived emission (Figure 4) supports the assignment of a short-lived MLCT state.

The TRVIS spectrum of ReAZBAP$^+$ recorded at 800 ps (Figure 3; ultrafast data) is similar to that at 11 ns (Figure 4; nanosecond data), showing that the spectrum of the longer-lived excited state comprises a broad feature at 400−600 nm with a sharper band at 500 nm. Nanosecond TRVIS spectra reported for [(bpy)Re(CO)$_3$(L)]$^+$ complexes where L contains a tertiary amine electron donor show bands at ca. 500 nm assigned to ligand-to-ligand charge-transfer (LLCT) states formed in accordance with Scheme 1.[13,22,30] Steady-state UV−visible spectra of organic tertiary amine compounds that have been chemically oxidized at the amine functionality show similar absorption bands at ca. 500 nm,[31] assigned to the $NR_2^{\bullet+}$ radical cation. Hence, the TRVIS spectrum of the longer-lived excited state of ReAZBAP$^+$ is assigned to the LLCT state, in which the azacrown has been oxidized to generate a $NR_2^{\bullet+}$ radical cation and the bipyridine ligand has been reduced, in accordance with Scheme 1. The nanosecond TRVIS kinetics indicate that this state has a lifetime of 19 ns,[32] providing further support for its assignment to an LLCT state: an ILCT state would be expected to have a much shorter lifetime because the ILCT state has a lifetime of <1 ns in the free amide−azacrown ligand.[32,33]

In summary, MLCT excitation of ReAZBAP$^+$ creates an excited MLCT state, [(bpy$^{\bullet-}$)Re^{II}(CO)$_3$(AZBAP)]$^+$, which undergoes forward electron transfer with a rate constant of $k_{FET} = 2.0 \times 10^9$ s^{-1} to create a charge-separated LLCT state, [(bpy$^{\bullet-}$)Re^{I}(CO)$_3$(AZBAP$^{\bullet+}$)]$^+$, which undergoes back electron transfer to the ground state with a rate constant of $k_{BET} = 5.3 \times 10^7$ s^{-1}. These processes are illustrated in Figure 5.

ReAZBAP$^+$−H$^+$ Photophysics. Protonation of the azacrown results in a substantial change in the photophysics of ReAZBAP$^+$ (Figures 3 and 4). By comparison with the data from ReBAP$^+$, all of the time-resolved absorption and emission data indicate that MLCT excitation of ReAZBAP$^+$−H$^+$ results in the formation of an MLCT excited state with a lifetime of 138 ns. The data reported here demonstrate that protonation of the azacrown nitrogen atom raises the energy of the LLCT state

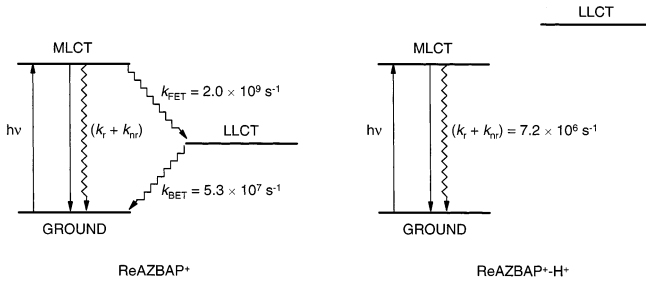

Figure 6. Schematic energy level diagrams and rate constants for ReAZBAP$^+$ and ReAZBAP$^+$−H$^+$. k_r and k_{nr} denote rate constants for radiative and nonradiative decay, respectively.

such that forward electron transfer does not occur in the MLCT state (Figure 6).

Forward Electron Transfer in ReAZBAP$^+$. The results presented here demonstrate that forward electron transfer in the MLCT state of ReAZBAP$^+$ is rapid, with the rate constant of $k_{FET} = 2.0 \times 10^9$ s^{-1} lying at the high end of the range of $k_{FET} = 10^7-10^9$ s^{-1} reported for analogous forward electron-transfer reactions of the type shown in Scheme 1 in related [(bpy)Re(CO)$_3$(L)]$^+$ complexes.[12,13,17,18,30] Forward electron transfer to create a charge-separated state on the picosecond time scale is a desirable property of a photochemical device.

The value of the rate constant for electron transfer can be expressed according to the semiclassical expression given in eq 1, which is appropriate for weakly exoergonic electron transfer in the high-temperature limit, and which can be applied to forward electron transfer in the MLCT state of ReAZBAP$^+$ at room temperature.[12,13,34] The rate constant, k_{et}, depends on the free energy for the process, ΔG, the total reorganization energy λ, comprising inner-sphere, λ_i, and outer-sphere, λ_o, contributions, and the electronic coupling, H_{AB}.

$$k_{et} = \frac{4\pi {H_{AB}}^2}{h(4\pi\lambda k_B T)^{1/2}} \exp\left(-\frac{(\Delta G + \lambda)^2}{4\lambda k_B T}\right) \qquad (1)$$

The free energy change for forward electron transfer in the MLCT state of ReAZBAP$^+$ has been estimated as $\Delta G = -0.14$ eV from electrochemical measurements.[22] The inner-sphere reorganization energy arises from changes in the equilibrium bond lengths of the azacrown electron donor, amide ligand connector, and (bpy$^{\bullet-}$)Re^{II}(CO)$_3$ electron acceptor groups.[2,13,34] Relatively large structural changes are expected on oxidation of the AZBAP ligand, and we estimate a contribution of 0.24 eV.[35] Relatively small structural changes are expected on reduction of the rhenium center in the MLCT state of ReAZBAP$^+$, and a contribution of <0.1 eV can be estimated.[42] Thus, the total inner-sphere reorganization energy of ReAZBAP$^+$ is estimated as $\lambda_i < 0.34$ eV.

The outer-sphere contribution arises from solvent reorientation and is typically estimated using a two-sphere model given by eq 2, where ϵ_{op} and ϵ_s are the optical and static dielectric constants of the solvent, respectively, r_A and r_D are the acceptor and donor radii, respectively, and r_{AD} is the acceptor−donor separation.[34]

$$\lambda_o = \frac{e^2}{4\pi\epsilon_0}\left(\frac{1}{\epsilon_{op}} - \frac{1}{\epsilon_s}\right)\left(\frac{1}{2r_A} + \frac{1}{2r_D} - \frac{1}{r_{AD}}\right) \qquad (2)$$

The acceptor radius in ReAZBAP$^+$ may be estimated as $r_A = 4.0$ Å,[13] and we estimate the donor radius as $r_D = 3.6$ Å and the acceptor−donor separation as $r_{AD} = 10.2$ Å.[35] Substituting these estimates into eq 2 yields a value of $\lambda_o = 1.26$ eV for the

outer sphere reorganization energy. Thus, the total reorganization energy is estimated to be $\lambda = (\lambda_i + \lambda_o) < 1.60$ eV. However, similar calculations on [(N−N)Re(CO)$_3$(L)]$^+$ complexes which undergo forward electron transfer according to Scheme 1 have given values 1.6 times larger than the experimental values,[13,17] and so a more reliable estimate for ReAZBAP$^+$ is $\lambda \approx 1.0$ eV. Taking these estimates of $\Delta G = -0.14$ eV and $\lambda \approx 1.0$ eV, it is evident that $-\Delta G \leq \lambda$ and that forward electron transfer in the MLCT state of ReAZBAP$^+$ occurs in the Marcus normal region.

Substituting the estimates of ΔG and λ, and the measured value of k_{FET}, into eq 1 gives an estimate of $H_{AB} \approx 13$ meV (100 cm^{-1}) for the donor−acceptor electronic coupling matrix element for forward electron transfer in the MLCT state of ReAZBAP$^+$. This estimated value of H_{AB} has a small uncertainty arising from the measured value of k_{FET} and a much larger uncertainty arising from the estimation of λ, with a relatively small increase in λ giving a large increase in the estimated value of H_{AB}.[44]

Back Electron Transfer in ReAZBAP$^+$. The rate constant of $k_{BET} = 5.3 \times 10^7$ s^{-1} for back electron transfer in the LLCT state of ReAZBAP$^+$ is significantly lower than the rate constant for forward electron transfer in the MLCT state, and it lies at the high end of the range of $k_{BET} = 10^6-10^7$ s^{-1} reported for analogous back electron transfers of the type shown in Scheme 1 for related [(bpy)Re(CO)$_3$(L)]$^+$ complexes.[13,17,30] It should be noted that the back electron transfer is a different reaction from the forward electron transfer, which creates the charge-separated state (Figure 5). Electrochemical measurements have shown that the combined oxidation of the reduced bipyridine, bpy$^{\bullet-}$, and reduction of the amine radical cation, $NR_2^{\bullet+}$, is strongly exoergonic, giving an estimated free energy change $\Delta G = -2.29$ eV for back electron transfer in the LLCT state of ReAZBAP$^+$.[22] The observation of a relatively low rate constant for this highly exoergonic reaction indicates that back electron transfer in the LLCT state of ReAZBAP$^+$ occurs in the Marcus inverted region, consistent with that reported for related [(bpy)Re(CO)$_3$(L)]$^+$ complexes.[13,17,30]

Effect of Molecular Design on Electron-Transfer Rates. Although the spectra and kinetics of the MLCT and LLCT states have not been reported previously for ReAZBAP$^+$, they have been reported for the analogous dimethylamino-substituted complex with a methylene spacer between the benzamide and pyridine groups, ReDMAB$^+$.[13] The MLCT and LLCT excited

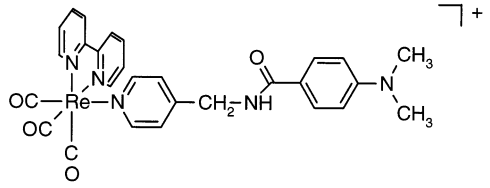

ReDMAB$^+$

states of ReDMAB$^+$ have longer lifetimes than those of ReAZBAP$^+$, decaying on the nanosecond time scale (Table 2) with rate constants of $k_{FET} = 8.6 \times 10^7$ s^{-1} and $k_{BET} = 1.3 \times 10^7$ s^{-1} obtained from time-resolved emission and nanosecond absorption measurements, respectively. The principal difference between these two complexes is the methylene spacer group present in ReDMAB$^+$, and it is useful to rationalize the difference in electron-transfer rate constants.

The rate constant for forward electron transfer in the MLCT state of ReAZBAP$^+$ is substantially (23 times) greater than that reported for ReDMAB$^+$. The electronic coupling, H_{AB}, decreases exponentially with donor−acceptor separation, as given by eq 3,[34] where $H_{AB(0)}$ is the coupling at the sum of their van der Waals radii, r_0, and β is a parameter that scales the coupling with separation.

$$H_{AB} = H_{AB(0)} \exp\left(-\frac{\beta}{2}(r - r_0)\right) \quad (3)$$

The values of $H_{AB(0)}$ can be assumed to be similar in ReAZBAP$^+$ and ReDMAB$^+$ because the (bpy$^{\bullet-}$)Re(CO)$_3$ acceptor groups are identical and the azacrown and dimethylamino donor groups, respectively, are similar. Using identical values of $H_{AB(0)}$ and substituting values of $H_{AB} = 100$ and 7 cm^{-1},[13] and through-bond distances of $r = 10.6$ and 12.1 Å,[35] which are appropriate for a super-exchange mechanism, for ReAZBAP$^+$ and ReDMAB$^+$, respectively, gives an estimated ratio for β of ca. 1.0:1.8. This ratio indicates that the attenuation of the electronic coupling with separation is significantly greater in a connecting group that includes a saturated methylene spacer and that both the donor−acceptor separation and the molecular design of the connecting group contribute to the occurrence of rapid forward electron transfer in the MLCT state of ReAZBAP$^+$.

The rate constant for back electron transfer in the LLCT state of ReAZBAP$^+$ is moderately (4 times) greater than that reported for ReDMAB$^+$. The larger separation between the bpy$^{\bullet-}$ donor and the $NR_2^{\bullet+}$ acceptor, and the additional presence of the rhenium metal within the connecting group, will result in a smaller value of H_{AB} than that for forward electron transfer in both complexes. It is evident that back electron transfer is less sensitive to the design of the connecting group than forward electron transfer. However, the rate constants for back electron transfer are not so easily rationalized as those for forward electron transfer because additional factors may be important: intersystem crossing may be required in returning to the ground state,[13] because the LLCT state forms rapidly from a ^{3}MLCT state and therefore may be more accurately described as a ^{3}LLCT state; and nuclear tunneling may be significant in the Marcus inverted region.[20]

The difference in electron-transfer rate constants between ReAZBAP$^+$ and ReDMAB$^+$ provides useful information on molecular design parameters for sensors and switches based on the general [(N−N)Re(CO)$_3$(L)]$^+$ design. The design of the donor−acceptor connecting group is clearly important in determining the rate of forward electron transfer but is less important in determining the rate of back electron transfer. The azacrown group within ReAZBAP$^+$ renders it useful as a sensor of protons or metal cations, and it has been proposed to release metal cations on excitation:[22] the results reported here demonstrate that ReAZBAP$^+$ has an appropriate design for a molecular switch because it has a connecting group that facilitates picosecond charge separation to form a charge-separated state that lives for nanoseconds.

Conclusions

We have demonstrated, by direct observation with time-resolved absorption spectroscopy, that forward electron transfer occurs in the MLCT excited state of ReAZBAP$^+$ to generate a charge-separated LLCT state. Forward electron transfer occurs on the picosecond time scale, and in the Marcus normal region, whereas back electron transfer occurs on the nanosecond time scale, and in the Marcus inverted region. This study provides quantitative evidence for a relatively long-lived LLCT excited state, as postulated by MacQueen and Schanze,[22] in which charge separation is effected between an azacrown ether and a bipyridine ligand attached to a rhenium metal center. In

particular, the creation of a radical cation at the nitrogen heteroatom of the azacrown offers clear opportunities for the development of light-controlled ion switches based on cation release from the azacrown on excitation.[22]

Acknowledgment. We acknowledge Professor R. E. Hester for assistance with the ultrafast measurements at LENS, and both LENS (supported by the European Community under contract HPRI-CT1999-00111) and EPSRC for financial support.

References and Notes

(1) Balzani, V., Ed. *Electron Transfer in Chemistry*; Wiley-VCH: Weinheim, 2001.

(2) Balzani, V.; Scandola, F. *Supramolecular Photochemistry*; Ellis Horwood Ltd.: London, 1991.

(3) De Cola, L.; Belser, P. *Coord. Chem. Rev.* **1998**, *177*, 301.

(4) Isied, S. S.; Vassilian, A. *J. Am. Chem. Soc.* **1984**, *106*, 1726.

(5) Isied, S. S.; Vassilian, A.; Magnuson, R. H.; Schwarz, H. *J. Am. Chem. Soc.* **1985**, *107*, 7432.

(6) Tapolsky, G.; Duesing, R.; Meyer, T. J. *Inorg. Chem.* **1990**, *29*, 2285.

(7) Frank, M.; Nieger, M.; Vogtle, F.; Belser, P.; von Zelewsky, A.; De Cola, L.; Balzani, V.; Barigelletti, F.; Flamigni, L. *Inorg. Chim. Acta* **1996**, *242*, 281.

(8) Encinas, S.; Bushell, K. L.; Couchman, S. M.; Jeffery, J. C.; Ward, M. D.; Flamigni, L.; Barigelletti, F. *J. Chem. Soc., Dalton Trans.* **2000**, 1783.

(9) Chen, P.; Curry, M.; Meyer, T. J. *Inorg. Chem.* **1988**, *28*, 2271.

(10) Schanze, K. S.; Sauer, K. *J. Am. Chem. Soc.* **1988**, *110*, 1180.

(11) Perkins, T. A.; Hauser, B. T.; Eyler, J. R.; Schanze, K. S. *J. Phys. Chem.* **1990**, *94*, 8745.

(12) Schanze, K. S.; Cabana, L. A. *J. Am. Chem. Soc.* **1990**, *94*, 2740.

(13) MacQueen, D. B.; Schanze, K. S. *J. Am. Chem. Soc.* **1991**, *113*, 7470.

(14) McGarrah, J. E.; Kim, Y.-J.; Hissler, M.; Eisenberg, R. *Inorg. Chem.* **2001**, *40*, 4510.

(15) Kalyanasundaram, K. *J. Chem. Soc., Faraday Trans. 2* **1986**, *82*, 2401.

(16) Stufkens, D. J.; Vlček, A., Jr. *Coord. Chem. Rev.* **1998**, *177*, 127.

(17) Schanze, K. S.; MacQueen, D. B.; Perkins, T. A.; Cabana, L. A. *Coord. Chem. Rev.* **1993**, *122*, 63.

(18) Wang, Y.; Lucia, L. A.; Schanze, K. S. *J. Phys. Chem.* **1995**, *99*, 1961.

(19) Lucia, L. A.; Wang, Y.; Nafisi, K.; Netzel, T. L.; Schanze, K. S. *J. Phys. Chem.* **1995**, *99*, 11801.

(20) Chen, P.; Duesing, R.; Graff, D. K.; Meyer, T. J. *J. Phys. Chem.* **1991**, *95*, 5850.

(21) Liard, D. J.; Vlček, A, Jr. *Inorg. Chem.* **2000**, *39*, 485.

(22) MacQueen, D. B.; Schanze, K. S. *J. Am. Chem. Soc.* **1991**, *113*, 6108.

(23) Lednev, I. K.; Hester, R. E.; Moore, J. N. *J. Am. Chem. Soc.* **1997**, *119*, 3456.

(24) Lednev, I. K.; Ye, T.-Q.; Hester, R. E.; Moore, J. N. *J. Phys. Chem. A* **1997**, *101*, 4966.

(25) Lednev, I. K.; Hester, R. E.; Moore, J. N. *J. Phys. Chem. A* **1997**, *101*, 7371.

(26) Lewis, J. D.; Perutz, R. N.; Moore, J. N. *Chem. Commun.* **2000**, 1865.

(27) Bussotti, L.; Foggi, P.; Gellini, C.; Moroni, L.; Salvi, P. R. *Phys. Chem. Chem. Phys.* **2001**, *3*, 3027.

(28) Neuwahl, F. V. R.; Bussotti, L.; Foggi, P. In *Research Advances in Photochemistry and Photobiology*; Global Research Network: Trivandrum, India, 2000; p 77.

(29) The UV−visible absorption spectrum of the free AZBAP ligand in acetonitrile has a similar profile to that of ReAZBAP$^+$, with a strong band at 324 nm ($\epsilon = 17\,000$ mol^{-1} dm^3 cm^{-1}) and weaker bands at ca. 250 nm.

(30) Wang, Y.; Schanze, K. S. *J. Phys. Chem.* **1996**, *100*, 5408.

(31) Hester, R. E.; Williams, K. P. J. *J. Chem. Soc., Perkin Trans. 2* **1982**, 559.

(32) Although excitation of ReAZBAP$^+$ at 355 nm (nanosecond experiments) populates both MLCT and ILCT states, the nanosecond data can be assigned to processes arising from population of the MLCT state: the nanosecond data are fully consistent with the ultrafast data (MLCT state excited exclusively at 400 nm), and they do not show any additional features arising from population of the ILCT state. Nanosecond studies of the free AZBAP ligand in acetonitrile show that its excited-state lifetime is <1 ns on excitation at 355 nm, into the ILCT band. Together, these data suggest that the ILCT state of ReAZBAP$^+$ is sufficiently short-lived to be unobserved with nanosecond time resolution.

(33) We have also obtained time-resolved resonance Raman spectra of ReAZBAP$^+$ that provide further evidence for the LLCT assignment, and against an ILCT assignment, from the positions of bpy and CO bands; these data will be reported elsewhere.

(34) Fox, M. A., Chanon, M., Eds. *Photoinduced electron transfer*; Elsevier: Amsterdam, 1988; Vol. 1.

(35) Semiempirical AM1 and DFT B3LYP/6-31G(d) calculations (Gaussian 98)[36] were performed on neutral and cation forms of a model AZBAP ligand in which the azacrown ether was replaced by a dimethylamino group. Ionization to the radical cation resulted in small changes at the amidopyridine and larger changes at the dimethylaminobenzene group, consistent with a semiquinoid structure[37−39] and with a change from partially pyramidal to planar geometry at the amine nitrogen.[40] The reorganization energy was calculated as 0.24 eV from the difference between the energy of the cation at its optimized geometry and at the optimized geometry of the neutral species (AM1); replacing the methyl groups with extended alkyl ether chains resulted in the same value. Distances were estimated as $r_D = 3.6$ Å for the radius of the (dimethylamino)benzamide donor, $r_{AD} = 10.2$ Å for the through-space distance from Re to the centre of the phenyl ring, and $r = 10.6$ and 12.1 Å for the through-bond distance from Re to the edge of the phenyl ring for model AZBAP and DMAB ligands, respectively (DFT; and using a Re−N bond length of 2.2 Å from crystallographic data[41]).

(36) Frisch, M. J.; Trucks, G. W.; Schlegel, H. B.; Scuseria, G. E.; Robb, M. A.; Cheeseman, J. R.; Zakrzewski, F. G.; Montgomery, J. A., Jr.; Stratmann, R. E.; Burant, J. C.; Dapprich, S.; Millam, J. M.; Daniels, A. D.; Kudin, K. N.; Strain, M. C.; Farkas, O.; Tomasi, J.; Barone, V.; Cossi, M.; Cammi, R.; Mennucci, B.; Pomelli, C.; Adamo, C.; Clifford, S.; Ochterski, J.; Petersson, G. A.; Ayala, P. Y.; Cui, Q.; Morokuma, K.; Malick, D. K.; Rabuck, A. D.; Raghavachari, K.; Foresman, J. B.; Cioslowski, J.; Ortiz, J. V.; Baboul, A. G.; Stefanov, B. B.; Liu, G.; Liashenko, A.; Piskorz, P.; Komaromi, I.; Gomperts, R.; Martin, R. L.; Fox, D. J.; Keith, T.; Al-Laham, M. A.; Peng, C. Y.; Nanayakkara, A.; Gonzalez, C.; Challacombe, M.; Gill, P. M. W.; Johnson, B.; Chen, W.; Wong, M. W.; Andres, J. L.; Gonzalez, C.; Head-Gordon, M.; Replogle, E. S.; Pople, J. A. *Gaussian 98*, revision A.7; Gaussian, Inc.: Pittsburgh, PA, 1998.

(37) Forster, M.; Hester, R. E. *J. Chem. Soc., Faraday Trans. 2* **1981**, *77*, 1535.

(38) Kwok, W. M.; Ma, C.; Matousek, P.; Parker, A. W.; Phillips, D.; Toner, W. T.; Towrie, M.; Umapathy, S. *J. Phys. Chem. A* **2001**, *105*, 984.

(39) Kwok, W. M.; Ma, C.; Phillips, D.; Matousek, P.; Parker, A. W.; Towrie, M. *J. Phys. Chem. A* **2000**, *104*, 4188.

(40) Brouwer, A. M.; Wilbrandt, R. *J. Phys. Chem.* **1996**, *100*, 9678.

(41) Yam, V. W.-W.; Lau, V. C.-Y.; Cheung, K.-K. J. *Chem. Soc., Chem. Commun.* **1995**, 259.

(42) The inner-sphere reorganization energy on reduction of the MLCT state of $[Ru(bpy)_3]^{2+}$ has been calculated as $\lambda_i < 0.1$ eV;[43] although the presence of strongly back-bonded CO ligands might be expected to give a higher value of λ_i, the applicability of this value to reduction in the MLCT state of $(bpy)Re(CO)_3L$ systems has been justified.[13]

(43) Toma, H. E.; Creutz, C. *Inorg. Chem.* **1977**, *16*, 545.

(44) If the calculated total reorganisation energy was 1.5 times larger than the experimental value, then $\lambda \approx 1.1$ eV and $H_{AB} \approx 22$ meV (180 cm^{-1}).